

Bone-free 3D Computed Tomography Angiography Using an Image-processing Application – Imaging Efficacy for Aneurysms Near the Skull Base and Clipped Cerebral Aneurysms

Noriaki Tomura,¹ Makoto Koga,² Takahiro Otani,³ Toshiaki Nishii⁴ and Satoshi Takahashi⁵

1. Associate Professor of Radiology, and Chief of Neuroradiology; 2. Research Associate in Radiology;

3. Assistant Professor of Radiology; 4. Research Associate in Radiology; 5. Lecturer in Radiology, Akita University School of Medicine

Abstract

Bone-free 3D computed tomography angiography (CTA) can be carried out to image cerebral aneurysms near the skull base when the elimination of bones is surgically required. The maximum intensity projection (MIP) images were initially obtained using the application. Further post-processing was performed to obtain the MIP and volume-rendering (VR) images. This technique did not increase radiation exposure to patients, and remnant bones in the initial MIP images automatically acquired by the application for bone elimination could be easily removed through post-processing. Although parts of vessels were sometimes removed from the image along with the bones, these could be quickly and easily recovered through post-processing. Thus, bone-free 3D CTA and conventional 3D CTA are complementary tools for imaging cerebral aneurysms near the skull base prior to surgery. This application could also eliminate clips in cases of clipped cerebral aneurysms, and it could improve the accuracy of detecting remnant necks after clipping surgery.

Keywords

Computed tomography angiography (CTA), cerebral aneurysm, skull base, bone-free CTA, clipping surgery

Disclosure: The authors have no conflicts of interest to declare.

Received: 18 June 2009 **Accepted:** 23 March 2010 **Citation:** *European Neurological Review*, 2010;5(1):103–6 DOI:10.17925/ENR.2010.05.01.103

Correspondence: Noriaki Tomura, Hospi-net Center, 6-1, Hiroomote Kawasaki, Akita City, Akita, 010-0041, Japan. E: tomura@cna.ne.jp

3D computed tomography angiography (3D CTA) is used to image cerebral aneurysms, steno-occlusive lesion of cerebral vessels and brain tumours. 3D CTA has become the accepted alternative to conventional intra-arterial digital subtraction angiography (IADSA) for imaging and detection of aneurysms^{1–5} and planning treatment. Multidetector (MD) CT allows a more precise evaluation of aneurysms with a shorter scanning time⁶ and better spatial resolution. Bony structures often disturb 3D CTA images near the skull base, and thus as a vessel-extraction technique, on the basis of the CT image registration, the subtraction of CT images of bony structures from CTA images has been developed,^{7–14} however, there are some limitations to this technique. For instance, subtle misregistration between the two CT images causes bone fractions in the subtracted images. More importantly, the two CT scans required for the technique expose the patient to two doses of radiation.

In an effort to address these concerns, a new image-processing application to eliminate bony structures and clipped cerebral aneurysms has been developed. This application has already been used for 3D CTA in patients with cerebral aneurysms near the skull base, and the efficacy of 3D CTA using this application for bone elimination has been evaluated.¹⁵ We also evaluated the efficacy of this technique in eliminating clip images in patients with clipped cerebral aneurysms.

Aneurysms

The cerebral aneurysms evaluated before surgery were determined to be located at the junction of the internal carotid artery (ICA) and the posterior communicating artery (IC-PC aneurysm), at the

paraclinoid part of the ICA (paraclinoid aneurysm), at the junction of the ICA and the anterior choroid artery (Acho aneurysm), at the cavernous segment of the ICA (cavernous aneurysm), at the junction of the ICA and the ophthalmic artery (IC-oph aneurysm), at the terminal portion of the ICA (IC terminal aneurysm) and at the basilar tip (basilar tip aneurysm). The cerebral clipped aneurysms evaluated were IC-PC aneurysms, paraclinoid aneurysms, aneurysms at the anterior communication arteries (AcomAs), aneurysms at the middle cerebral arteries (MCAs), basilar tip aneurysms and aneurysms at the vertebral artery (VA). All of these were clipped using titanium clips.

Computed Tomography Scanning

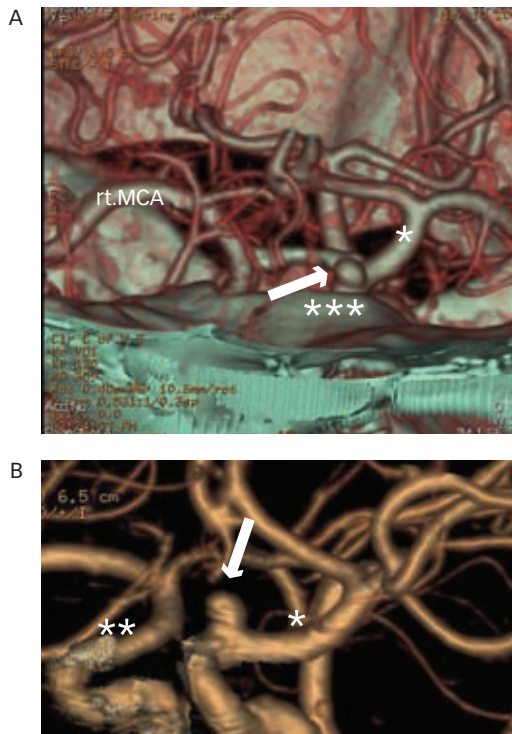
At our hospital, CT was performed with 64 (GE Healthcare, LightSpeed VCT, Milwaukee, WI) or 32 detector rows (GE Healthcare, LightSpeed Pro 32), 120kV, Z-axis automatic tube current modulation (AutomA) ($\leq 600\text{mA}$), a 0.625mm-section thickness, a field of view (FOV) of 25cm and a scanning time of 0.4 seconds per rotation. The scan range per rotation was 20mm (LightSpeed Pro 32) or 40mm (LightSpeed VCT). Non-ionic contrast medium (350 or 370mgI/ml) was injected using a power injector via a 20-gauge needle in the antecubital vein using a test-injection technique¹⁶ or an automatic trigger system. As a test injection, 10ml of contrast medium was injected at a rate of 4ml/second. A reference slice was used to monitor a region of interest in the cervical portion of the ICA to detect the arrival of contrast medium after injection. The proper delay was determined and the right or left common carotid artery was used as the reference point for the automatic trigger system. Acquisition of images started following the appropriate delay after injection of contrast medium. A total of 50ml

Figure 1: Cavernous Aneurysm of the Internal Carotid Artery



An anterior-to-posterior view of a volume-rendered (VR) image with the application for bone elimination clearly shows a cavernous aneurysm (white arrows) of the left internal carotid artery (ICA). The single white asterisk indicates the ICA on the left side, and the double white asterisks indicate the ICA on the right side.

Figure 2: Paraclinoid Aneurysm of the Left Internal Carotid Artery



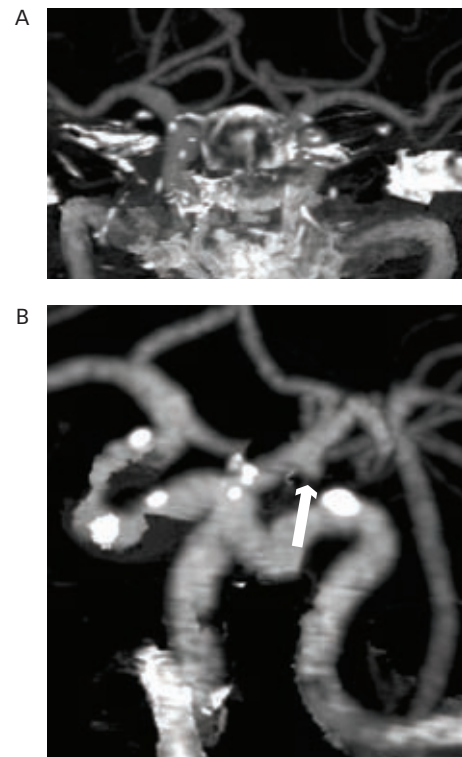
A: An anterior-to-posterior view of a volume-rendered (VR) image by conventional 3D computed tomography angiography (3D CTA) shows a paraclinoid aneurysm (white arrow) of the left internal carotid artery (ICA) close to the lesser wing of the sphenoid bone. The single white asterisk indicates the left ICA. The triple white asterisks indicate the lesser wing of the sphenoid bone. B: A left anterior oblique view of the VR image with the application for bone elimination clearly shows a paraclinoid aneurysm of the left ICA (white arrow). The single white asterisk indicates the left ICA, and the double white asterisks indicate the right ICA.

of contrast medium was administered at a rate of 4ml/second. Axial CT data were transferred to a 3D imaging workstation (Advantage Workstation, GE Healthcare).

Image Processing and Results Aneurysm Imaged Before Surgery

A maximum intensity projection (MIP) image was first automatically obtained using the application for bone elimination (AutoBone Xpress, GE Healthcare Technologies) without any manual post-processing, taking approximately 20 seconds to obtain the first MIP images. The

Figure 3: Aneurysm at the Junction of the Internal Carotid Artery and the Posterior Communicating Artery

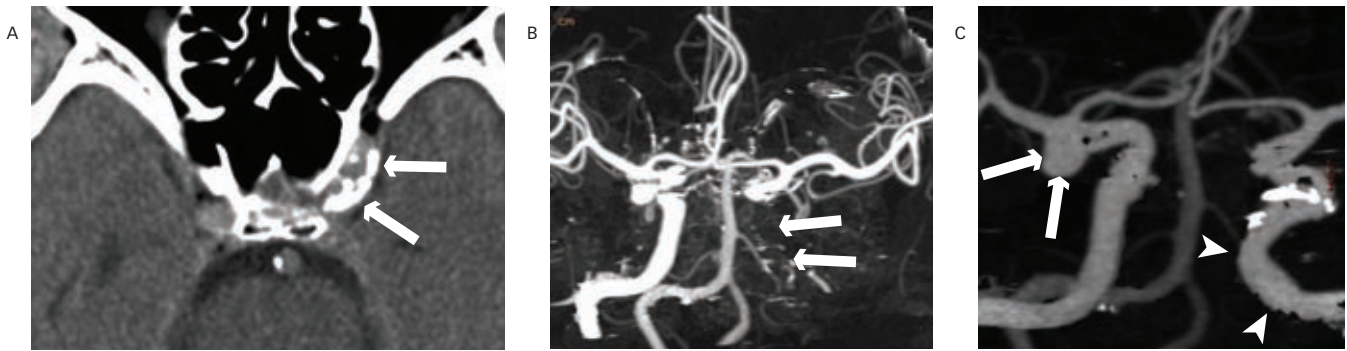


A: An anterior-to-posterior view of the initial maximum intensity projection (MIP) image by the application for bone elimination shows dense bone remnants. B: A left anterior oblique view of the volume-rendered (VR) image after post-processing clearly shows an internal carotid-posterior communicating artery (IC-PC) aneurysm (white arrow).

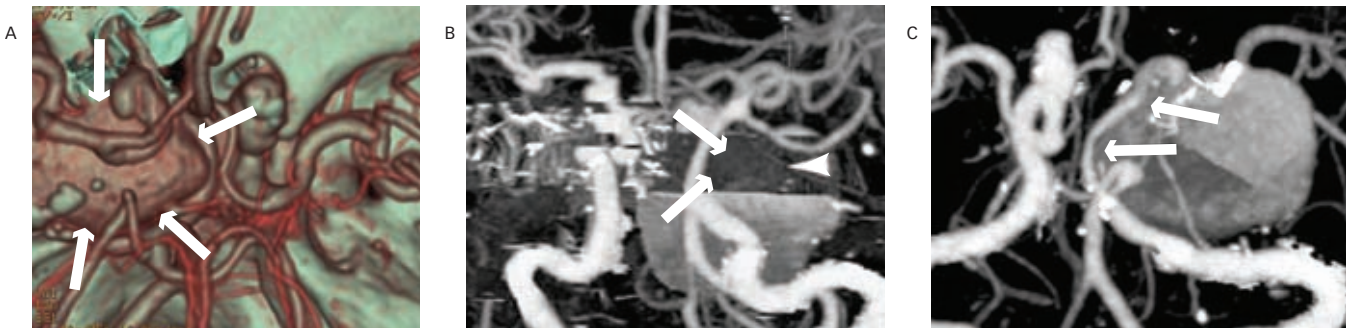
theory of bone elimination using this application has been reported previously.¹⁷ Volume-rendered (VR) images were obtained after the MIP images had been acquired (see *Figures 1* and *2*), and when almost no residual bone was visible, no further processing was necessary; however, approximately 80% of the patients required additional processing. Small bone remnants, which did not interfere with the image of the ICA or basilar artery, were visible near the ICA or basilar artery in approximately 50% of the patients and were easily removed from the image. Large bone remnants of the sphenoid and/or petrous bones were seen in approximately 10% of the patients; these were also able to be removed in this study (see *Figure 3*). Removal of part of the ICA siphon was most often seen due to dense calcification of the siphon of the ICA. When there was any dense calcification of an arterial wall in locations other than the siphon of the ICA, part of the relevant artery was also automatically removed by the application. However, further post-processing was able to recover all loss of the ICA image (see *Figure 4*). In a few cases part of the siphon of the ICA without calcification was removed by the application, although the mechanism is unclear. In cases with giant aneurysms with a wide neck, part of the parent arteries were removed because the giant aneurysms were not filled with contrast medium. In such cases, the parent arteries could be imaged after post-processing (see *Figure 5*). In our study, there was a significant difference in the visualisation of aneurysms and their necks between VR images processed with and without the application for bone elimination.¹⁵

Clipped Aneurysms

This application automatically removed the titanium clip images from the majority of aneurysms clipped with a single clip imaged using 3D

Figure 4: Aneurysm at the Terminal Portion of the Internal Carotid Artery

A: Non-contrast-enhanced computed tomography (CT) image shows dense calcification of the left internal carotid artery (ICA) (white arrows). Although all of the left ICA is removed on the anterior-to-posterior view of the initial maximum intensity projection (MIP) image by the application for bone elimination (white arrows) (B), a left anterior oblique view of the MIP image after post-processing shows complete recovery of the image of the left ICA (white arrowheads) and depicts the aneurysm at the terminal portion of the right ICA (white arrows) (C).

Figure 5: Giant Cavernous Aneurysm of the Internal Carotid Artery

A: A superior view of conventional 3D computed tomography angiography (3D CTA) shows only part of the cavernous aneurysm (white arrows). B: An anterior-to-posterior view of the initial maximum intensity projection (MIP) image by the application for bone elimination shows incomplete filling of contrast medium in the aneurysm (arrowhead) and non-filling of the cavernous segment of the left ICA (white arrows). C: An anterior-to-posterior view of the MIP image after post-processing depicts the cavernous segment of the left ICA (white arrows) (C).

CTA (see *Figure 6*). Some post-processing was usually necessary to remove any remaining bones at the cranial base. Conventional 3D CTA sometimes overlooks remnant necks that are obscured by clips, and, if necessary, we were able to quickly and easily recreate the clips. In our study, when neck remnants of clipped aneurysms were present, 3D CTA with clip elimination was able to clearly visualise the neck remnants (see *Figure 7*). However, in aneurysms involving triple or quadruple clips, the metal artefacts obscured the presence or absence of the neck remnants.

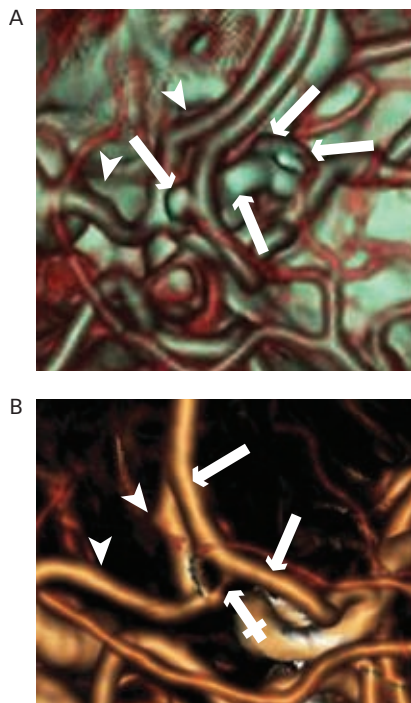
Discussion

To date, a digital subtraction technique has usually been used to eliminate bones from CT images. This subtraction technique requires accurate registration during the entire acquisition, before and after contrast administration. In this case, a stereotactic frame to prevent movement of the head is used during data acquisition; however, this is uncomfortable for the patient. Moreover, the subtraction technique has the major disadvantage of requiring two scans, thus increasing the exposure of the patient to radiation. By contrast, the current method uses an image-processing application to eliminate bone structures at the base of the skull, instead of a subtraction technique. The current technique requires only one scan and therefore exposes the patient to a lower dose of radiation. Another advantage is a reduction of the time required to manually remove bony structures from images. The initial MIP images were automatically obtained within approximately 20 seconds. In the majority of cases, the remnant bones were small, only a few were near the ICA or basilar artery and most did not

interfere with the ICA or basilar artery images. Remnant bones were easily removed from images through post-processing. Moreover, in the few cases in which large bone remnants were seen, these were easily removed through post-processing.

This technique has the major disadvantage of partial loss of vessel images on the initial MIP image. However, all images exhibiting a loss of vessels can be fully recovered through further post-processing. During post-processing, care must be taken in terms of the existence of small aneurysms at the site of the recovered artery and the site of remnant bone removal. This technique of employing an image-processing application for bone elimination is much more feasible for imaging aneurysms compared with conventional 3D CTA with bony structures. However, information regarding bony structures is critical for neurosurgeons prior to surgery; therefore, bone-free and conventional 3D CTA are complementary tools for imaging cerebral aneurysms before surgery. The current application for elimination of bones can also eliminate clips in cases of clipped cerebral aneurysms. Recognition of a residual aneurysm neck on post-operative angiography is of paramount importance, because incomplete treatment of an aneurysm may result in recurrent haemorrhage with serious or fatal consequences.^{18,19} There have been cases of small neck remnants re-growing over a long period into a dangerous aneurysm. IADSA has usually been used to evaluate clip placement in patients with clipped cerebral aneurysms; however, there have been a few previous reports suggesting the feasibility of 3D CTA after clipping surgery for cerebral aneurysms.^{20,21} These studies evaluated the use of

Figure 6: Clipped Aneurysm at the Anterior Communicating Artery



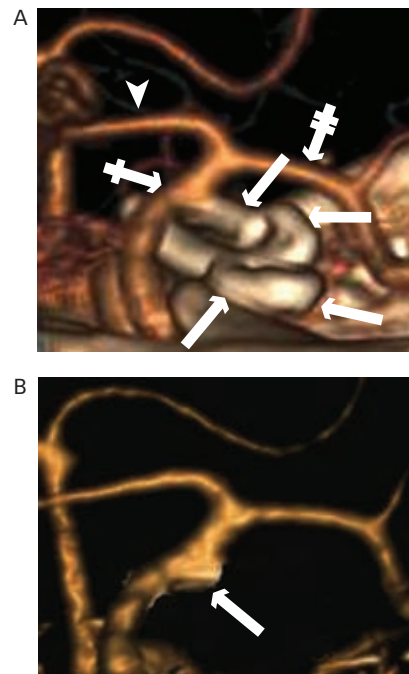
A: A superior oblique view of a conventional 3D computed tomography angiography (3D CTA) image shows a clip at the anterior communication artery (AcomA), and does not clearly depict whether or not there are any remnant necks (white arrows, clip; white arrowheads, right anterior cerebral artery). B: A left anterior oblique view of the volume-rendered (VR) image by the application for bone elimination clearly depicts no remnant neck (white arrows, left anterior cerebral artery; white arrowheads, right anterior cerebral artery; single crossed white arrow, AcomA) of the aneurysm without a clip.

conventional 3D CTA with clips to replace IADSA, but 3D CTA with clip elimination could be significantly superior to conventional 3D CTA. 3D CTA using MDCT has the potential to replace IADSA to confirm complete or incomplete clipping of cerebral aneurysms in cases involving no more than one or two clips. MR angiography (MRA) also provides 2D and 3D images of aneurysms without bony structures. There are several limitations in imaging aneurysms by MRA.²² Flow-related artefacts can result in under-estimation of the size of aneurysms. Even in larger aneurysms, turbulent flow and/or thrombosis within the aneurysm can cause poor visualisation of the aneurysm by MRA. However, MRA using 3 Tesla (3T) MR systems is able to clearly image small aneurysms.^{23–25} Further studies should compare the current bone-free CTA technique with MRA. Moreover, to determine whether bone-free 3D CTA is a viable alternative to IADSA, detection of aneurysms should also be compared between 3D CTA and IADSA in a blinded study.

Conclusion

Bone-free 3D CTA using an image-processing application for the elimination of bones can improve delineation of cerebral aneurysms

Figure 7: Clipped Aneurysms at the Internal Carotid Posterior Communicating Arteries and at the Junction of the Anterior Choroid Artery and Internal Carotid Artery



A left anterior oblique view of a conventional 3D computed tomography angiography (3D CTA) image (A) does not clearly show the remnant neck due to clips at the IC-PC (white arrows, clips; white arrowheads, left anterior cerebral artery; single crossed white arrow, left ICA; double crossed white arrow, left middle cerebral artery). A left anterior oblique view of the volume-rendered (VR) image (B) by the application for bone elimination clearly depicts a small part of a remnant neck (white arrow) of the aneurysm without clips.

near the skull base. This technique does not increase radiation exposure to patients, and remnant bones in the initial MIP images automatically acquired by the application for bone elimination can be easily removed through post-processing. Although parts of vessels are sometimes removed from the image along with the bones, these can be quickly and easily recovered through post-processing.

Thus, bone-free 3D CTA and conventional 3D CTA are complementary tools for imaging cerebral aneurysms near the skull base prior to surgery. This application can also eliminate clips in cases of clipped cerebral aneurysms. 3D CTA with the elimination of clips can improve the accuracy of detecting remnant necks after clipping surgery, and may be a viable alternative to IADSA for the detection of remnant necks in cases with single or double clips. ■

Noriaki Tomura is an Associate Professor of Radiology and Chief of Neuroradiology at Akita University. He is board-certified in radiology and nuclear medicine, and received his MD from Akita University. His research interests are primarily in diagnostic neurology, head and neck radiology and nuclear medicine of the brain.

- Kouskouras C, et al., *Neuroradiology*, 2004;46: 842–50.
- Uysal E, et al., *Diagn Interv Radiol*, 2005;11:77–82.
- Pechlivanis I, et al., *Acta Neurochir (Wien)*, 2005;147:1045–53.
- Tipper G, et al., *Clin Radiol*, 2005;60:565–72.
- Kato Y, et al., *Acta Neurochir*, 2002;144:715–22.
- Agid R, et al., *Neuroradiology*, 2006;48:787–94.
- Venema HW, et al., *Radiology*, 2001;218:893–8.
- Moore EA, et al., *Eur Radiol*, 2001;11:137–41.
- Jayakrishnan VK, et al., *AJNR Am J Neuroradiol*, 2003;24:451–5.
- Abrahams JM, et al., *Neurosurgery*, 2002;51:264–9.
- Kwon SM, et al., *Comput Med Imag Graph*, 2004;28:391–400.
- van Straten M, et al., *Am Assoc Phys Med*, 2004;31:2924–33.
- Tomandl BF, et al., *AJNR Am J Neuroradiol*, 2006;27:55–9.
- Sakamoto S, et al., *AJNR Am J Neuroradiol*, 2006;27: 1332–7.
- Tomura N, et al., *Jpn J Radiol*, 2009;27:31–6.
- Sasiadek M, et al., *Med Sci Monit*, 2002;8:MT99–104.
- Suryanarayanan S, et al., *Image Processing*, 2004;5370:410–19.
- Lin T, et al., *J Neurosurg*, 1989;70:556–60.
- Sasaki T, et al., *J Neurosurg*, 1994;80:58–63.
- Dehdashti AR, et al., *J Neurosurg*, 2006;104:395–403.
- Tomura N, et al., *Clin Radiol*, 2006;61:505–12.
- Gailoud P, et al., *Neuroradiology*, 2003;45:404–9.
- Villablanca JP, Saleh R, *AJNR Am J Neuroradiol*, 2006;27:2118–21.
- PH, Hui F, Sitoh YY, *Ann Acad Med Singapore*, 2007;36:388–93.
- Miki H, Kiriyaama I, *Magn Reson Med Sci*, 2008;7:169–78.